# Experimental and Finite Element Modeling of Self Compacted Reinforced Concrete Beams Strengthened by Bottom Steel Plates

**Jamal A. Farhan**[1] **Zaydon M. Ali**[2]

(Received 24/4/2013; accepted 25/6/2013)


## Abstract

In this study, eight rectangular reinforced concrete beams strengthened by bottom steel plates firmly interconnected to them by headed-stud shear connectors are manufactured using self compacting concrete and tested up to failure under two point loads to demonstrate the effect of steel-plate thicknesses, lengths, and the shear-connector distributions on the behavior, ductility and strength of this type of beams. A trial mix conforming to the EFNARC Constraints had been successfully carried out to satisfy the three fresh tests of SCC, these tests are flowability, passing ability and segregation resistance.

The results show that there is a substantial improvement in the flexural resistance, increasing the flexural stiffness and decreasing the ductility ratio due to thickening steel plate, On contrary, increasing the spacing between shear connectors to 50% had slight effect on the flexural resistance, but subsequent increase of their spacing to 100% had seriously lowered that resistance, The spacing between shear connectors has a primary effect on the average flexural stiffness and ductility ratio. In regard to the steel plate length, its shortening has reduced the flexural resistance significantly, decreased the average flexural stiffness and had increased the ductility ratio.

The experimentally determined ultimate flexural strength had been compared with its corresponding one computed by the "Strength Method" using ACI requirements where high agreement gained between them due to the nearly perfect interaction provided by SCC.

The eight composite beams had also been analyzed by the non-linear three dimensional Finite Element Analysis employing ANSYS program (release 12.1),where high agreement is achieved compared with experimental results.


Keywords: Composite SPCC beams, Finite elements, Partial interaction, Self Compacted (SCC) Concrete , ANSYS

# النمذجة العملية وبطريقة العناصر المحددة للعتبات الخرسانية المسلحة ذاتية الرص والمقواة بصفائح معدنية من الأسفل

جمال عبدالواحد فرحان زيدون محسن علي


## الخلاصة

في هذه الدراسة تم إنشاء ثمان عتبات خرسانية مسلحة مقواة بصفائح حديدية من الأسفل مربوطة بروابط قصية باستخدام خرسانة ذاتية الرص وتحميلها لحد الفشل تحت تاثير حملين مركزين لدراسة تاثير سمك الصفيحة وطولها وكذلك توزيع الروابط القصية على تصرف ومقاومة ومطاوعة هذا النوع من العتبات . كما تم انتاج عدة خلطات تجريبية مطابقة للمواصفات الاوربية EFNARC لتحقيق الفحوصات الطرية للخرسانة ذاتية الرص، هذه الفحوصات هي فحص الانتشار، فحص قابلية المرور خلال التسليح الكثيف وفحص مقاومة الانعزال .



[1] *Assistant professor at the Department of civil Engineering , Anbar University.*

[2] *Student at the Department of civil Engineering , Anbar University.*

بينت النتائج أن زيادة سمك الصفيحة يحسن من مقاومة الانثناء بشكل واضح ويرافقه تحسن في صلابة الانثناء ولكنه يقلل من نسبة المطاوعة. إما بالنسبة للروابط القصية فان تقليلها بنسبة 50% له تأثير قليل على مقاومة الانثناء لكن زيادة المسافة بين الروابط القصية بنسبة لاحقة 100% قللت المقاومة بشكل كبير.
كما بينت النتائج ان زيادة المسافة بين الروابط القصية له تأثير رئيسي على صلابة الانثناء عند الفشل AFS وعلى نسبة المطاوعة وإن نقصان طول الصفيحة قلل من مقاومة الانثناء بصورة ملحوظة كذلك قلل من قيمة صلابة الانثناء وأدى إلى زيادة نسبة المطاوعة.
كذلك تمت في هذه الدراسة مقارنة مقاومة الانثناء القصوى المحسوبة عمليا مع مقاومة الانثناء المناظرة لها المحسوبة باستخدام "طريقة المقاومة" حسب متطلبات معهد الخرسانة الأمريكي ACI وتبين ان هناك تقارب كبير في النتائج وذلك بسبب الربط الجيد الذي حققته الخرسانة ذاتية الرص.
تم تحليل هذه العتبات المركبة الثانية نظريا باستخدام التحليل اللاخطي ثلاثي الأبعاد بطريقة العناصر المحددة باستخدام برنامج ANSYS (إصدار 12.1) وتم الحصول على توافق عالي بين النتائج العملية والنظرية.

# 1. Introduction

This type of composite beams is called steel plate- concrete composite beams (SPCC) as shown in Fig.1. There are many advantages of the SPCC structures which are, there is no concrete cover outside the steel plate, so the weight of the structure can be reduced, and there is no crack exposed at the bottom of the structures and the steel plate can be used as formwork during construction. On other hand, the using of self compacting concrete in this type of composite beams increase the degree of interaction between steel plate and concrete due to homogenous dispersion of SCC mix around shear connectors.

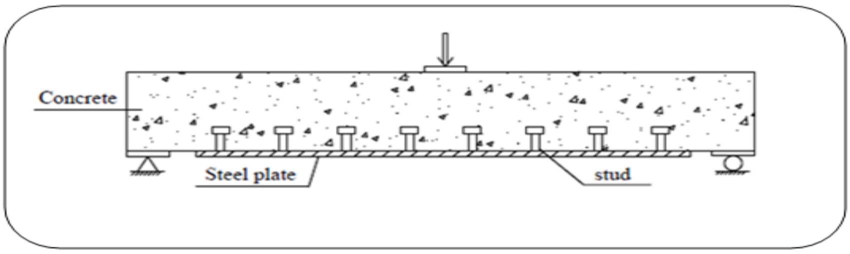


Fig.1: Steel Plate Concrete Composite Beam

There are many advantages of SCC Including: easier placing, reduction in site manpower ,Improved durability, better surface finishes , reduced noise levels and absence of vibration[1].

A literature review reveals that a few number of studies was performed on SPCC beams. The beginning was in 1989 due to Roberts and Haji-Kazemi[2]. Test results showed a significant improvement in the stiffness of the plated beams, and all beams exhibited a ductile failure followed by crushing of the concrete in the compression zone. In 1997, Abtan[3] conducted tests on twelve specimens to investigate the behavior of SPCC beams. The variables were lengths, widths and thicknesses of steel plate. The test results showed that external reinforcement (plates) increases flexural stiffness of the beam at all stages of loading, and, consequently, reduces the deflection at corresponding loads. Less deflection was obtained with increasing the length and area of plate. In 2000, Al-Saraj(4) presented a theoretical study for reinforced concrete beams strengthened mechanically by external steel plates attached to their tension side with so called “Shear Connector” by using finite difference method. Slip, deflections, stress and strain have been calculated by previously tests. Close agreements are obtained with the experimental values for different thickness and widths of the strengthening plates. In 2009, tests were carried out by Jianguo Nie and Jie Zhao[5] on five specimens in order to investigate the flexural behavior of SPCC beams. Based on test results, steel plate and concrete can work together very well and the SPCC beams have a very good ductility. The ultimate strength of the SPCC beams can be calculated by means of the same plastic method as reinforced concrete beams.

The SCC was first developed in Japan in the 1980'S to enhance the durability of concrete structures. Since then, several investigations have been carried out to achieve a rational mix design for this type of concrete, which is comparable to normal concrete. In 1995, Okamura and Ozawa[6] proposed a simple proportioning system as follows: The coarse aggregate content in concrete is fixed at 50% of the solid volume. The fine aggregate content is fixed at 40% of the mortar volume. The water-powder ratio by volume is assumed as 0.9 to 1.0, depending on the properties of the powder. The superplasticizer dosage and final water-powder ratio are determined so as to ensure self-compactability. In 2002, EFNARC[1] put the guidelines of the typical range of materials used in SCC and these guidelines were modified in 2005 by EFNARC again as shown in Table 1.

Table 1: Typical range of SCC mix composition[1]

| Constituent $Kg/m^3$ | Powder | Water | Gravel | Sand | Water/powder (by volume) |
|---|---|---|---|---|---|
| Typical range($kg/m^3$) | 380-600 | 150-210 | 750-1000 | 48-55% of total aggregate weight. | 0.85-1.10 |

The specification of proportion mix must be satisfy three properties ,filling ability, passing ability and segregation resistance. The test methods of these properties and typical acceptance criteria for SCC with a maximum aggregate size up to 20 mm that used in the present study are shown in Table 2.

Table 2:Test methods for workability properties of SCC[1]

| Method | Property | Typical range of values |
|---|---|---|
| 1- Slump flow by Abrams cone (mm) | Filling ability | 650-800 |
| 2- $T_{50cm}$ slump flow(sec) | Filling ability | 2-5 |
| 3- J-ring (mm) | Passing ability | 0-10 |
| 4- V-funnel (sec) | Filling ability | 6-12 |
| 5- V-funnel at $T_{5minutes}$ (sec) | Segregation resistance | 0-3(Max) |

# EXPERIMENTAL PROGRAM

## DESCRIPTION OF BEAMS

The tested beams are simply supported ones of 1200mm span, cross section (100 *150), shear connectors (studs) are 8 mm diameter and 37 mm height for all tested beams. Connectors have been placed at uniform spacing along the centerline of steel plate. The full details of beams and the parameters are presented in Table 3 and in Fig.2

Table 3: Details of the tested composite beams

| No. of Beam | B1 | B2 | B3 | B4 | B5 | B6 | B7 | B8 |
|---|---|---|---|---|---|---|---|---|
| Steel Plate thickness(t) | 3 | 4.75 | 6 | 8 | 4.75 | 4.75 | 6 | 6 |
| Spacing between studs(S) | 60 | 60 | 60 | 60 | 90 | 120 | 60 | 60 |
| Steel plate length (Lsp) (mm) | 1200 | 1200 | 1200 | 1200 | 1200 | 1200 | 960 | 720 |

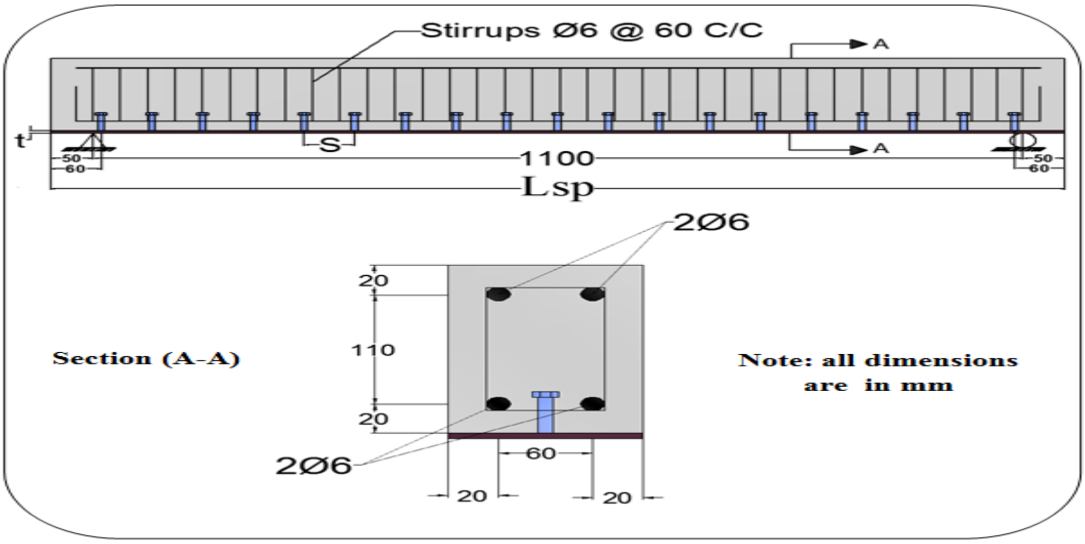


Fig. 2: Description of beams

# MATERIALS

## CEMENT

Ordinary Portland Cement (OPC) produced at AL-SHEMALIYA company, Kingdom of Saudi Arabia was used in this work. The chemical and physical tests were carried out in FALLUJA Cement Factory and the results indicate that the adopted cement conforms to the Iraqi specification No.5/1984[7]. Table 4 show the chemical test of cement.

## AGGREGATE

Al-Ramadi west region natural sand was used as a fine aggregate. On the other hand, Crushed gravel of 10 mm maximum size from AL-NEBAI region was used as a coarse aggregate. The grading and specifications of them are within Iraqi specifications No.45/1984[8].

## SUPER PLASTICIZER

To achieve the high workability needed to produce the self-compacting concrete, super plasticizer (Glenium 51) is used. It is relative density 1.1, at 20°C, PH=6.6[9].

## LIMESTONE POWDER

This material is locally named as "Al-Ghubra" which has been brought from the local market and used to increase the amount of powder (cement & filler). Table 4 shows the chemical composition of limestone powder.

## SILICA FUME

A grey-coloured densified silica fume is a pozzolanic material which has a high content of amorphous silicon dioxide and consists of very fine spherical particles. Table 4 shows the chemical composition of silica fume.

Table 4: Chemical properties of cementitious material

| Oxide Composition | | Cao | $SiO_2$ | $Al_2O_3$ | $Fe_2O_3$ | $SO_3$ | MgO | L.O.I | $K_2O$ | $Na_2O_3$ |
|---|---|---|---|---|---|---|---|---|---|---|
| Content | Cement | 62.2 | 22 | 5.2 | 3.1 | 3.1 | 2.4 | 2.4 | 1.2 | ------ |
| | Silica fume | 0.28 | 94.2 | 0.3 | 0.82 | 0.9 | 0.13 | 3.38 | 0.44 | 0.08 |
| | Limestone | 56.1 | 1.38 | 0.72 | 1.38 | 0.21 | 0.13 | 40.56 | ------ | ------ |

## Steel Material

6 mm steel bars have been used for all types of reinforcement with fy= 684.2 and E=210000, while different thicknesses of steel plate have been used for the tested beams with fy=422and E=190600. Studs of 8mm diameter and 37mm overall length were used as shear connectors for all composite beams with fy=350and E=207500.

## Mix Design of SCC

According to EFNARC specifications[1], several trial mixes are carried out in the laboratory to satisfy SCC requirements. The proportions of trial mix used in this work are as shown in Table 5.

Table 5: The proportions of trial mix

| material | Cement(kg/m$^3$) | Sand(kg/m$^3$) | Gravel(kg/m$^3$) | Water(kg/m$^3$) | GL51(lit/m$^3$) | SF(kg/m$^3$) | LSP(kg/m$^3$) |
|---|---|---|---|---|---|---|---|
| Amount | 332.5 | 900 | 750 | 170 | 10.5 | 17.5 | 150 |

# Testing of Fresh Concrete [1]

Slump flow and (T50cm) tests: The slump flow test is used to evaluate workability or filling ability. To evaluate filing ability ,two factors are measured. The first is (D-final) which is calculated by measuring the two perpendicular diameters of spread concrete and the second factor is T50 cm (the time consumed for the concrete to reach the 50cm spread circle is recorded). Fig. 3 illustrated slump flow test.

V-funnel test: V-funnel, see Fig.4 is used to measure the filling ability(Tv) and segregation resistance (Tv after 5 min). The value of TV is the time representing the ability of the concrete to flow out of the funnel. while TV5 value represents the same ability but after refilling the funnel and allowing concrete to flow after 5 minutes from the refilling.

J-ring test: The j-ring test is used to evaluate the passing ability. the BJ represent the J-ring value which is determined from the difference in height of concrete between the inside and outside of the J-Ring. Fig. 5 illustrated slump flow test.

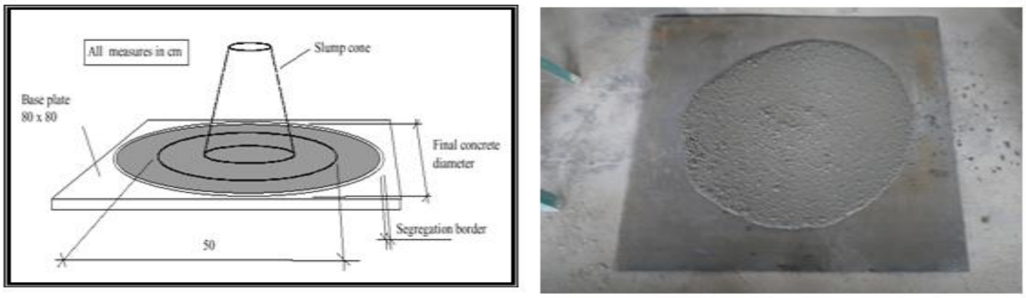


Fig. 3: Slump flow test[1]

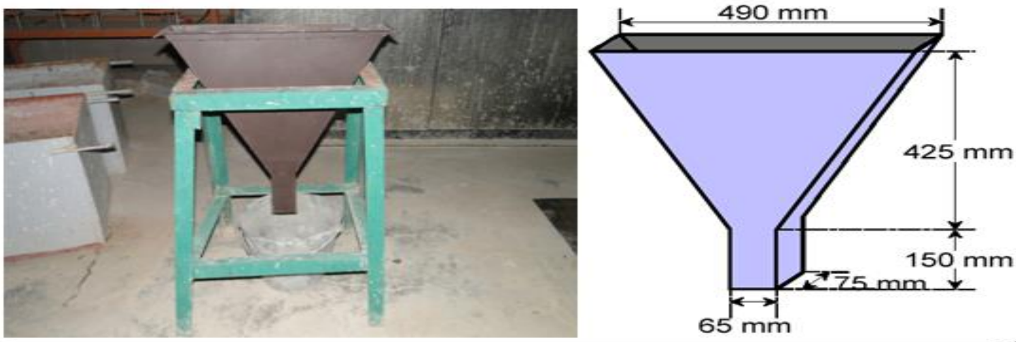


Fig. 4: V-funnel test details[1]

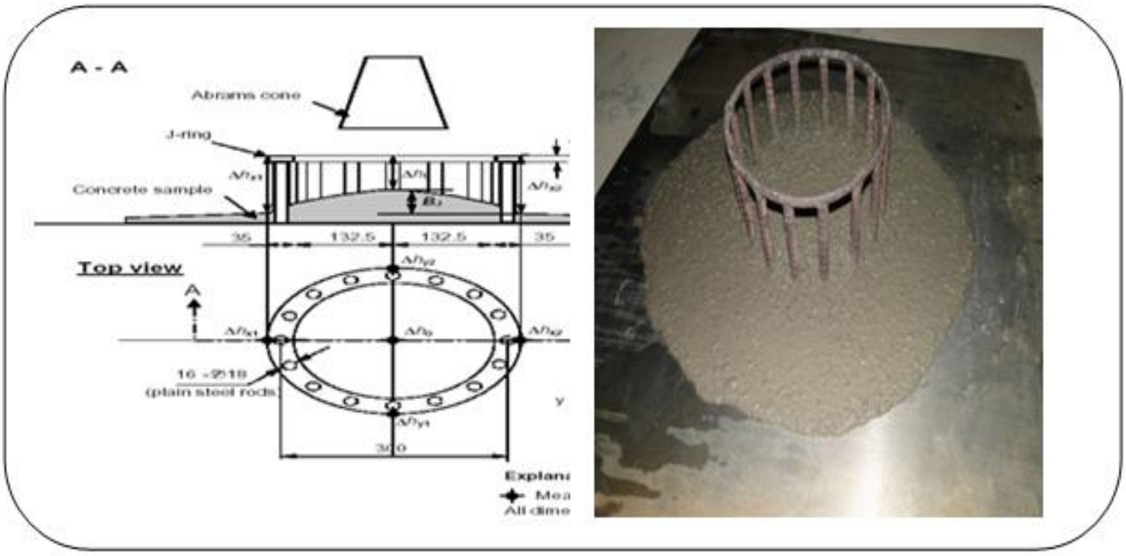


Fig. 5: J-ring test details[1]

## STRENGTH OF CONCRETE

Three cylindrical specimens, (150×300) mm, were used to determine the uniaxial compressive strength (fc'), tested according to ASTM C39-86[10]. On the other hand, the flexural strength test was conducted on (100*100*500) mm prisms. Two points load where used in this test according to ASTM C293-86 [11]. Table 6 shows the compressive and flexural strength of concrete for each mix.

Table 6: Compressive and tensile strength values of the tested beams

| Beam No. | $f_c'$ (MPa) | $f_t$ (MPa) |
|---|---|---|
| Beams 1,2&3 | 36 | 6.48 |
| Beams 4&5 | 35.6 | 6.39 |
| Beams 6,7&8 | 33.65 | 6.225 |

## PUSH OUT TEST

One Push-out test prototype was fabricated and prepared according to BS 5400[12] to evaluate the strength of one shear connector as shown in plate 1. Table 7 shows the results of push out test.

Plate 1: Push-out test machine

Table 7: Load ~slip relationship for one shear connector

| Load(kN) | 0 | 4.62 | 18.05 | 27.55 | 36.1 |
|---|---|---|---|---|---|
| Slip(mm) | 0 | 0.4 | 1.61 | 2.58 | 4.1 |

## BEAM FABRICATION, CASTING OF CONCRETE AND TESTING PROCEDURE

The tested beams are fabricated into steel formwork as shown in plate 2. Then, The concrete mixtures were casted in the formwork. After twenty four hours from casting, the formworks were removed, then, submerged in a water tank for 28 days to be ready for test.

Plate 2: beams fabrication

All beams have been tested at an age of 28 days. A 400 kN-capacity hydraulic testing machine was used to test the beams at the Mechanical Engineering Laboratory at the University of Anbar. Fig 6 and plate 3 explain the instrumentation and the testing apparatus.

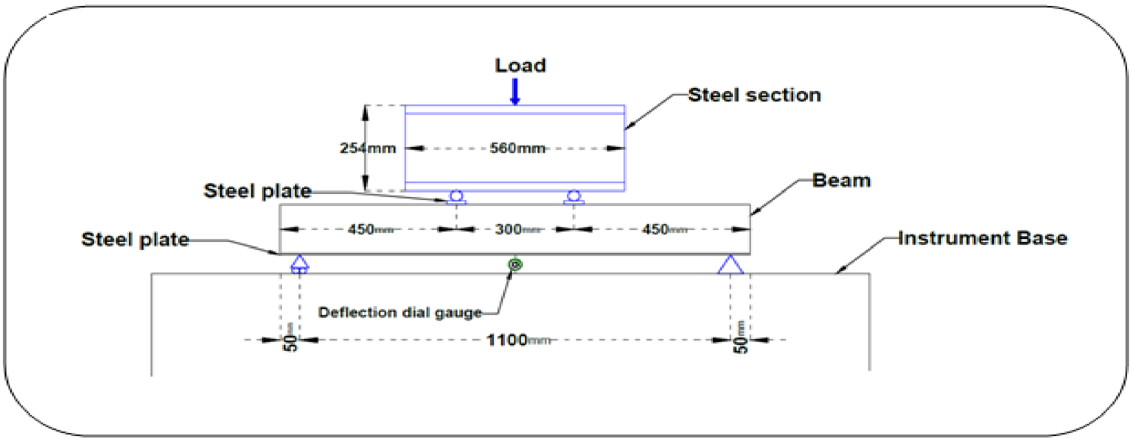


Fig. 6: Schematic diagram of the test arrangement


Plate 3: The testing apparatus

A load cell and a dial gauge were used to read the load and measure the mid span deflection, respectively. The dial gauge was placed directly under the centerline of the beam in order to record the mid-span deflection at every load stage. The testing continued until the failure of beams occurred.

# RESULTS AND DISCUSSION

## FRESH PROPERTIES OF SCC

The properties of fresh concrete mixture were investigated in the laboratory to achieve SCC requirement, their results were compared with EFNARC constraints[13]as shown in Table 8.

Based on observation and results, SCC has good workability, viscosity, no segregation or blocking has occurred and the filling ability in obstacle corner is very good.

Table 8: Test results of fresh concrete

| Type of test | Slump flow | | V-Funnel | | J-ring |
|---|---|---|---|---|---|
| | D(mm) | T50(sec) | Tv(sec) | $Tv_5$(sec) | $B_J$ (mm) |
| Result | 740 | 3 | 11 | 14 | 10 |
| Limitation[1] | 650-800 | 2-5 | 6-12 | Tv+3sec (Max) | 0-10 |

## PRESENTATION AND DISCUSSION OF THE TESTED BEAMS RESULTS

The measured responses for the tested beams have been represented by the load ~ mid-span deflection relationships given in Fig 6. Furthermore, numerical evaluations of the fundamental parameters reflecting flexural behavior have been evaluated and presented in Table 9. Based on the observed and the calculated results as shown in Table 9 and the modes of failure shown in plate 4 , the following two primary phenomena are discussed: a)Mode of failure. b) Flexural behavior.

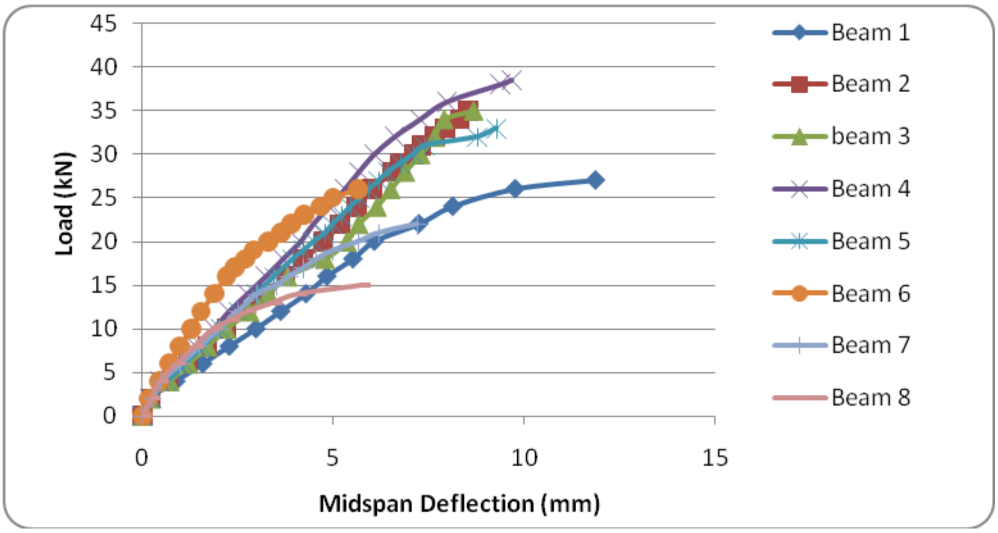


Fig 6: Load ~midspan deflection curves for all tested beams

Table 9 : Numerical values for the parameters of the flexural behavior

| Beam no. | Beam 1 | Beam 2 | Beam 3 | Beam 4 | Beam 5 | Beam 6 | Beam 7 | Beam8 |
|---|---|---|---|---|---|---|---|---|
| $P_{cr}$ (kN) | 17.7 | 22.11 | 24.63 | 28.2 | 21.8 | 21.15 | 15.05 | 15.2 |
| $\Delta_{cr}$ (mm) | 1.25 | 1.3 | 1.43 | 1.51 | 1.18 | 0.7 | 0.5 | 0.43 |
| $P_u$ (kN) | 102.6 | 133 | 136.8 | 146.3 | 125.4 | 98.8 | 83.6 | 57 |
| $\Delta_u$ (mm) | 12 | 8.53 | 8.9 | 9.67 | 9.2 | 6 | 7.2 | 5.7 |
| AFS (kN/mm) | 8.55 | 15.6 | 15.37 | 15.13 | 13.63 | 16.46 | 11.61 | 10 |
| Ductility ratio | 9.6 | 6.56 | 6.22 | 6.4 | 7.8 | 8.57 | 14.4 | 13.25 |

## MODE OF FAILURE

Based on plate 4 , beam of minimum steel plate thickness(Beam1) failed in bending, and the subsequent increase in that thickness causes diagonal shear failure . Decreasing the degree of partial interaction (by incessant increases of the shear-connector spacing of Beam2 to 50% and 100% to get Beam5 and 6 ,respectively) does not affect the type of fracture pattern. Subsequent shortenings of the steel plate thickness of Beam3 by 20% and 40% to get Beams 7 and 8, respectively lead to combined (shear and bending) failure in the shear spans.

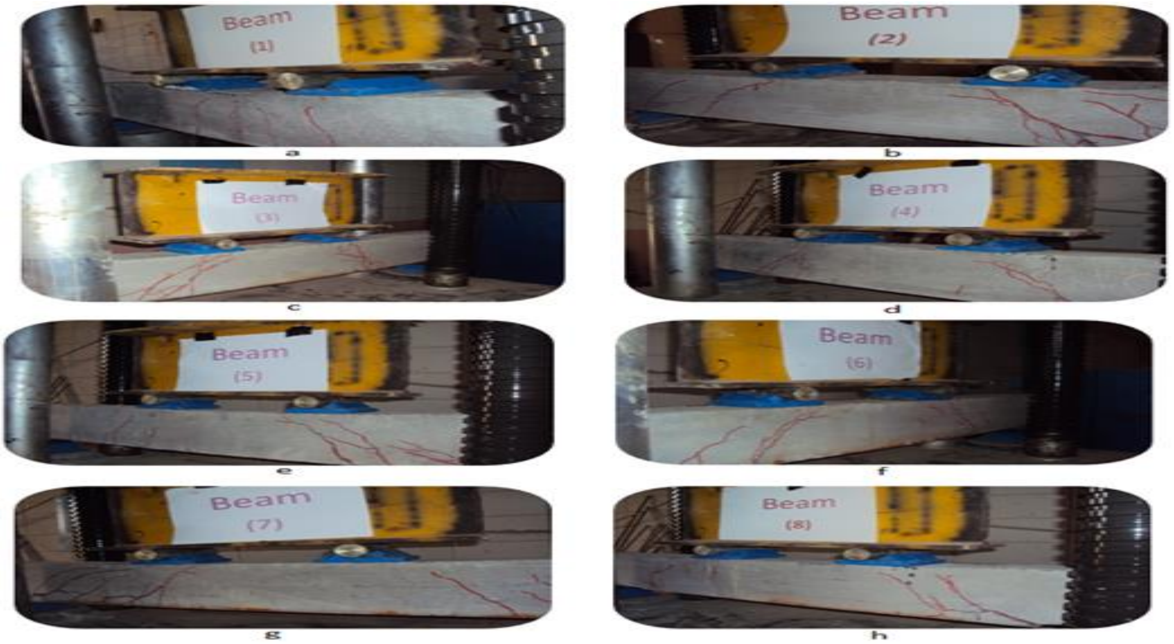


Plate 4: Fracture patterns at failure for the eight tested beams

# Flexural Behavior

## Ultimate load capacity

Steel plate thickness: based on Table 9, the increases of the steel plate thickness of Beam1 by 58.3% , 100% and 166% (to create Beams 2, 3 and 4, respectively) have produced an increases in the ultimate load values equal to 29.62% , 33.33% and 42.6% respectively.

Spacing of headed studs: On inspection of the variations (presented in Table 9) in the ultimate load values among Beams 2, 5 and 6 (where Beams 5 and 6 have an increase in the spacing of the shear connectors by 50 % and 100% , respectively relative to Beam2 ), it can be noticed that the reductions in the ultimate load values are 5.71 % and 25.71%, for Beams 5 and 6, respectively.

Steel plate length: studying the ultimate load Pu values presented in Table 9 for the eight tested beams clarifies the effect of decreasing the steel plate length of Beam3 by 20% and 40% to create Beam7 and 8, respectively led to respective percentage reductions of 38.88% and 58.33% in the ultimate load values

## Average flexural stiffness (AFS)

It can be recognized from Table 9 that increasing steel plate thickness from 3mm (Beam1) to 4.75mm (Beam2) had lead to a quantitative increase in the AFS parameter value by 82.45%. However; the additional two consecutive steps of increase in the bottom steel plate thickness 6mm and 8mm (for Beam3 and Beam4, respectively) have negligible effects on it . A gain , the degree of partial interaction has a secondary effect on AFS value, in the first stage of decreasing, the decrease in AFS for Beam5 (which has a 50% decrease in that degree relative to BEAM2) where only 12.62%, the effect of the additional 50% decrease in that degree(for Beam6) where 5.22%. Shortening the steel plate for Beam3 by 20% (to get Beam7) decreases AFS value by 24.46% , while the additional 40% shortening(to get Beam8) has negligible effect on AFS value(relative to the latter case).

## Ductility ratio:

EFFECT OF THE STEEL PLATE THICKNESS: The increase of the steel plate thickness of Beam1 by 58.3%,100% and 166% to represent Beam2, Beam3 and Beam4, respectively has decreased the value of the ductility ratio with maximum percent equal to 33.33%. The behavior can be explained as follows: Increasing the steel plate thickness actually reduces the possibility of the steel plate yielding, hence failure may occur by crushing the concrete in the compression zone or diagonal shear cracking of the concrete across beam depth causing less deflection.

EFFECT OF THE HEADED-STUD SPACING: The two increases of this spacing from 60 mm (Beam2) to 90mm then to 120 mm (for Beam6 and Beam9, respectively) are accompanied by increases in the initial value of the ductility ratio because of the whole yielding of steel plate with excessive deformation of headed stud.

EFFECT OF THE STEEL PLATE LENGTH: Finally, the two decreases of steel plate length of Beam3 by 20% then by 40% (to create Beam7 then Beam8, respectively ) have further increased the original value of the ductility ratio.

## Experimental evaluation of the partial interaction

To experimentally investigate degrees of the partial interaction at the steel-concrete interfaces of the eight tested beams ,their ultimate flexural strengths have been theoretically calculated (assuming perfect bond at the interfaces specified above) then compared with ultimate load values obtained experimentally. The ultimate flexural strength values have been calculated by means of the simplified plastic method according to ACI requirements[13]. The results for Beams 1 to 8 are shown in Table 10, which illustrates the high degree of interaction for the tested beams where full connection is achieved by the headed studs due to using Self Compacting Concrete which has Good flow and effective spread around the headed studs, thus producing almost a perfect bonding. Moreover, no segregation has occurred in the bottom of the beam (interface zone between the steel plate and the abutting concrete). Therefore, homogeneous mixes have been achieved by this type of concrete.

Table 10: Experimental and theoretical ultimate load

| Beam NO. | | Beam1 | Beam2 | Beam3 | Beam4 | Beam5 | Beam6 | Beam7 | Beam 8 |
|---|---|---|---|---|---|---|---|---|---|
| Ultimate load (kN) | Exp.* | 102.6 | 133 | 136.8 | 146.3 | 125.4 | 98.8 | 83.6 | 57 |
| | Theo.** | 82.8 | 123.06 | 139.4 | 147.06 | 124.28 | 122.17 | 137.27 | 137.27 |
| | Exp/Theo | 1.24 | 1.08 | 0.98 | 0.99 | 1.01 | 0.81 | 0.62 | 0.41 |

# Finite element modelling

A nonlinear finite element analysis of composite beams strengthened by bottom steel firmly interconnected to it by headed-stud shear connectors has been presented employing ANSYS computer program (Realease12.1) by using eight-node isoparametric brick elements for concrete, four node shell elements for steel plate, two node axial elements for reinforcing bar and interface elements to represent the bond between the steel plate and concrete.

# ELEMENT TYPE, REAL CONSTANT AND MATERIAL PROPERTIES

Characters of the finite element types used in modeling each of the eight tested beams by ANSYS program were summarized in Table 11. The real constants required the geometrical properties of the used elements, while the material properties require the behavior and characteristics of constitutive materials. The parameters used in the real constants and the material properties, and their numerical values are shown in Table 12 for Beam1 and with the same fashion for the seven remaining beams.

Table 11: Description of used elements[14]

| Beam components | | Used element from ANSYS library | Representation of element |
|---|---|---|---|
| Concrete | | SOLID65 | 8-node Brick Element (3 Translation DOF per node) |
| Steel reinforcement (longitudinal reinforcement ,diagonal shear reinforcement & shear connectors outside interface) | | LINK8 | 2-node Discrete Element (3 Translation DOF per node) |
| Steel plate | | SHELL63 | 4-node shell Element (3 Translation DOF per node & 3 Rotation DOF per node ) |
| Interface | Shear Friction and Contact | CONTA174& TARGE170 | Nonlinear Surface-to-Surface Interface Element |
| | Dowel Action ( shear connectors inside interface ) | COMBIN39 | 2-node zero length Nonlinear spring element with one Translation DOF per node |

# MODELING AND MESHING OF THE CONCRETE MEDIA, THE STEEL PLATES, AND REINFORCING BAR

The concrete prism (SOLID65) is formed by specifying coordinates of that prism, then its width, height and depth, while the steel plate(SHELL63) is initiated by introducing keypoints with respect to the origin of coordinates, then formation of the area is bounded by those keypoints. After creating the concrete media volume and the steel plate area, the finite element model requires their meshing. the rectangular mesh is used by dividing the concrete prism into small hexa-hydron brick elements of 10mm orthogonal side dimensions

Table 12: Parameters of the present finite element model and their numerical values for Beam1

<table>
<tr><th>Element</th><th>Parameter</th><th colspan="4">Definition</th><th colspan="2">Value</th></tr>
<tr><td rowspan="9">SOLID65</td><td>$f_c'$</td><td colspan="4">Ultimate compressive strength(MPa)</td><td colspan="2">37</td></tr>
<tr><td>$f_t$</td><td colspan="4">Ultimate tensile strength(MPa)</td><td colspan="2">6.48</td></tr>
<tr><td>$\beta_o$</td><td colspan="4" rowspan="2">Shear transfer parameters</td><td colspan="2">0.22</td></tr>
<tr><td>$\beta_c$</td><td colspan="2">0.2</td></tr>
<tr><td>$E_c$</td><td colspan="4">Young's modulus of elasticity(MPa)</td><td colspan="2">28200</td></tr>
<tr><td>$\upsilon$</td><td colspan="4">Poisson's ratio ²</td><td colspan="2">0.2</td></tr>
<tr><td colspan="7">Stress-strain relationship for concrete</td></tr>
<tr><td>Stress(MPa)</td><td>0.0</td><td>10. 8</td><td>22.58</td><td>30.37</td><td>34.92</td><td>36</td></tr>
<tr><td>Strain</td><td>0.0</td><td>0.000383</td><td>.0009</td><td>.0014</td><td>.002</td><td>.00255</td></tr>
<tr><td rowspan="5">LINK8</td><td>parameter</td><td colspan="4">Definition</td><td colspan="2">value</td></tr>
<tr><td>$A_b$</td><td colspan="4">Area of reinforcement( mm²) for Ø6</td><td colspan="2">28.6</td></tr>
<tr><td>$F_x$</td><td colspan="4">Yield stress(MPa) Tensile</td><td colspan="2">684.2</td></tr>
<tr><td>Es</td><td colspan="4">Modulus of elasticity(MPa)</td><td colspan="2">210000</td></tr>
<tr><td>$\upsilon$</td><td colspan="4">Poisson's ratio</td><td colspan="2">0.3</td></tr>
<tr><td rowspan="5">SHELL63</td><td>parameter</td><td colspan="4">Definition</td><td colspan="2">value</td></tr>
<tr><td>t</td><td colspan="4">Thickness of Shell63(mm)</td><td colspan="2">3 mm</td></tr>
<tr><td>$F_x$</td><td colspan="4">Tensile yield stress(MPa)</td><td colspan="2">420</td></tr>
<tr><td>Es</td><td colspan="4">Modulus of elasticity(MPa)</td><td colspan="2">190600</td></tr>
<tr><td>$\upsilon$</td><td colspan="4">Poisson's ratio</td><td colspan="2">0.3</td></tr>
<tr><td rowspan="2">CONTA170 & TARGE173</td><td>parameter</td><td colspan="4">Definition</td><td colspan="2">value</td></tr>
<tr><td>µ</td><td colspan="4">Coefficient of friction</td><td colspan="2">0.7</td></tr>
<tr><td rowspan="3">COMBIN 39</td><td colspan="7">Load–slip relationship for non linear spring elements (COMBINE39)</td></tr>
<tr><td>Load (kN)</td><td>0</td><td>4.62</td><td>18.05</td><td>27.55</td><td colspan="2">36.1</td></tr>
<tr><td>Slip (mm)</td><td>0</td><td>0.4</td><td>1.61</td><td>2.58</td><td colspan="2">4.1</td></tr>
</table>

while the steel plate is divided into rectangular shell element of 10 mm side dimension as shown in Fig.7.

Modeling of the steel bars(LINK8) is initiated by introducing keypoints then defining straight lines between those keypoints. The same fashion used for the concrete prism and the steel plate is used for the meshing reinforcing steel bar where 10 mm length elements are used. See Fig 7.

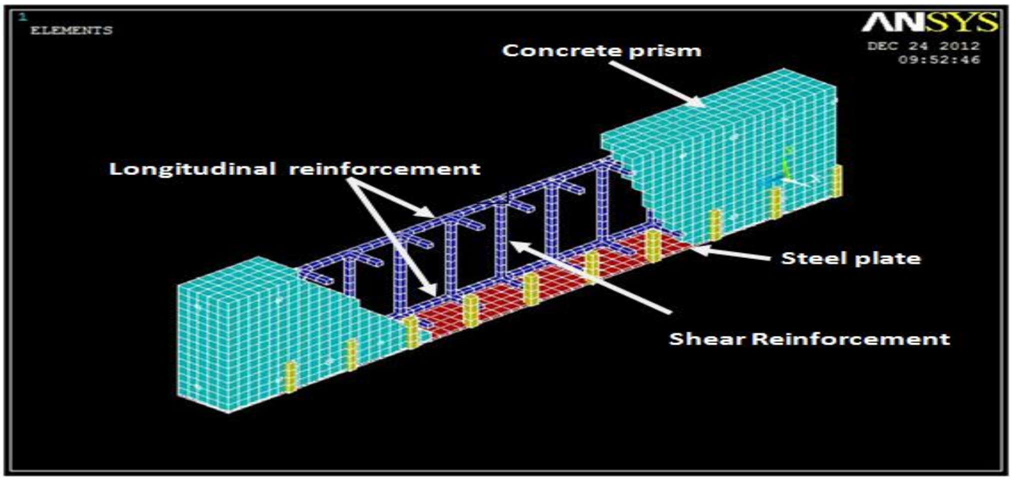


Fig. 7 Modeling and meshing of concrete prism, steel plate , the reinforcing bar and Interface modeling

To represent the friction between the concrete prism and the steel plate, contact pair "surface to surface" elements designated by TARGE170 and CONTA174 are used. For contact surface between the steel plate and the concrete prism beam, no mesh is needed because individual elements are created in the modeling through the surfaces created by the concrete volumes for CONTA174 and steel plate areas for TARGE170. In addition, spring element COMBIN39 is used to resist the slip while the uplift separation is resisted by the discrete element LINK8. These elements have been used to model the behavior of the shear connector, as shown in Fig 8 for Beam1, with the same manner for the seven remaining beams. COMBIN39 is created through the nodes between the concrete prism SOLID65 and steel plate SHELL63 in the interface plane, those nodes correspond to the nodes for TARGE170 and CONTA174. See Fig 8.

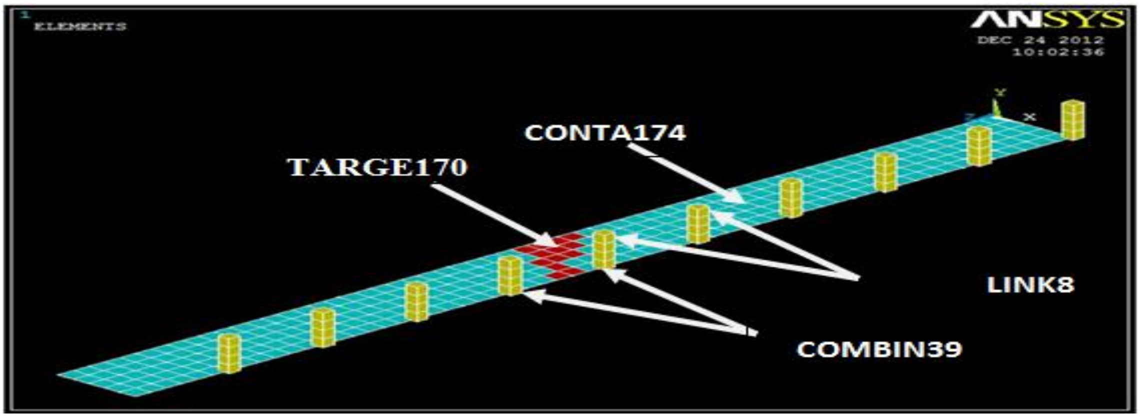


Fig 8: Modeling of the interface by the three ANSYS finite elements CONTA174, TARGE174 and COMBIN39

## BOUNDARY CONDITIONS, SIMPLE SUPPORT AND APPLIED LOAD

Due to double symmetries of the beams ,one quarter is taken. To model the symmetry, the displacement in the direction perpendicular to that plane is restrained (i.e Ux=Uz=0), therefore the constraining of two planes of symmetry must be applied in x- and z-directions.

The simple support is modeled by constraining a single line of nodes along the width of the beam soffit at 50 mm distance from the edge of the beam in the y- and z-direction (i.e Uz =Uy=0) as shown in Fig 9.

For external load, a quarter of the total load is applied to a quarter of the modeled beam at 450 mm from the beam edge (150 mm from the origin of coordinate ).It is distributed on the single line of nodes across the width of the top surface of the beam as shown in Fig 9.

## PRESENTATION OF THE ANSYS MODEL RESULTS

Results of the modeled beams by ANSYS computer program are represented by the load~mid-span deflection relationships and the predicted deformed shapes as shown in Fig 10 and Fig 11, respectively.

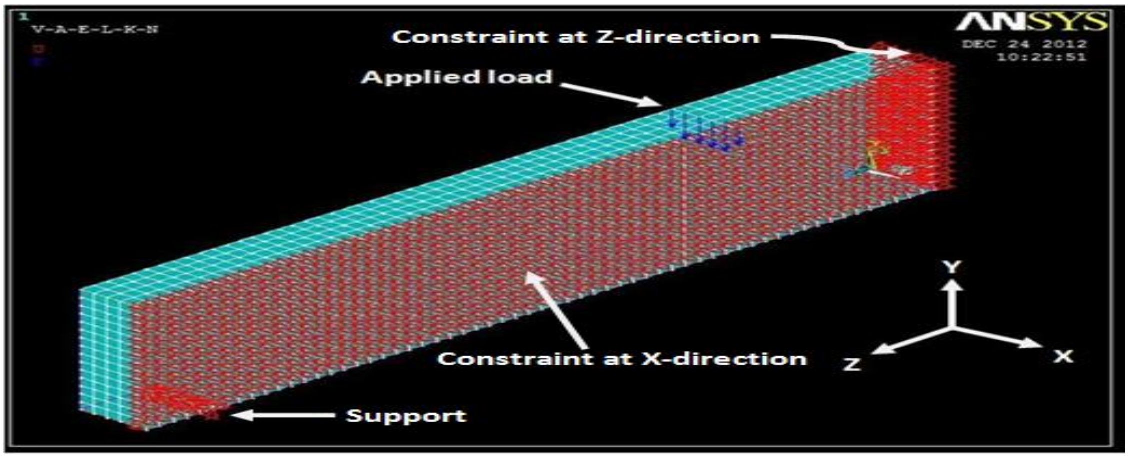


Fig 9: Boundary conditions, simple support and applied load

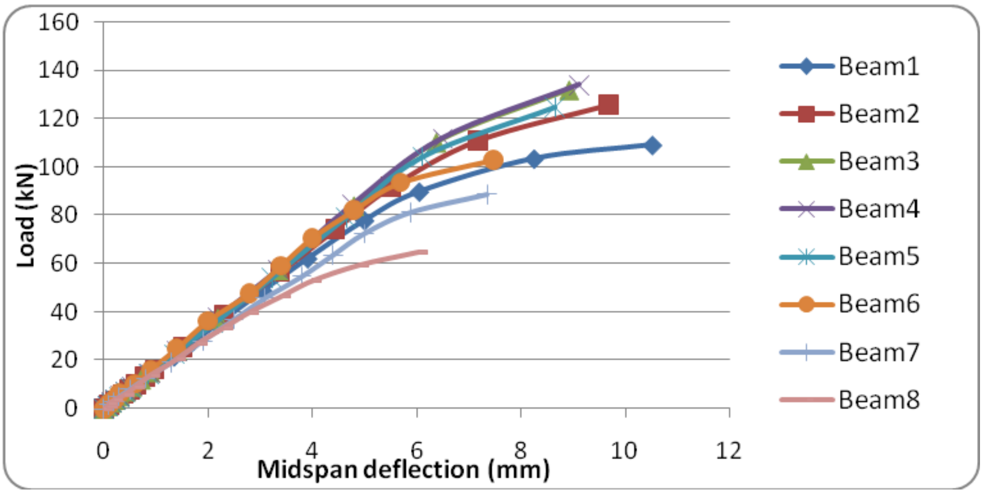


Fig 10: Load~midspan deflection relationships for the eight tested beams given by the present finite element by ANSYS program

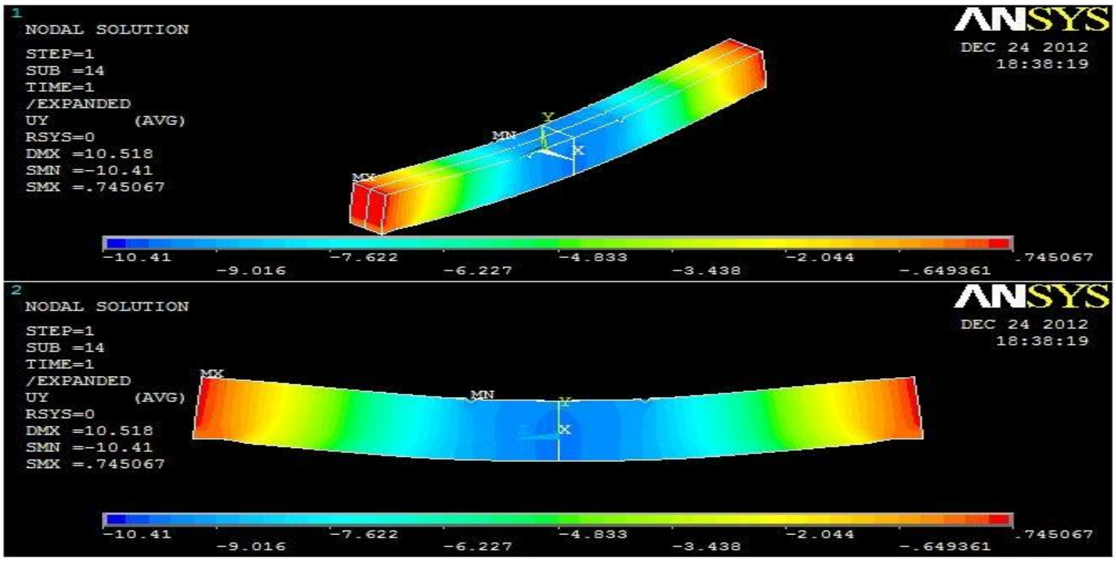


Fig 11: Deformed shape at ultimate stage predicted by the present ANSYS model

## CORRELATION BETWEEN THE EXPERIMENTAL AND NUMERICAL MODEL RESULTS

Results of the load~midspan deflection relationships obtained from the present ANSYS model are compared with the experimental load~midspan deflection ones. Good agreement can be observed in this comparison between ANSYS model results and the experimental ones presented in Table 13 and Fig 12.

Based on Table 13, it can be noticed the following:

a) The maximum absolute difference percentage of the ultimate load values is noticed in Beam8 where a value of 13.6% is detected.

b) The average percentage difference for the ultimate load values of eight beams is only 6.04 %.

c) The maximum percentage difference between the experimental and ANSYS model values of the mid-span deflection at the ultimate stage is 24.81% for Beam6.

d) However, the corresponding average percentage difference of the mid-span deflection at ultimate stage is 8.84%.

Table 13: Numerical values of the ultimate loads and the maximum midspan deflections for experimental and ANSYS model results and their difference percentages

| Modeled Beams | Ultimate load $P_u$ (KN) | | | Mid span deflection $\Delta_u$(mm) | | |
|---|---|---|---|---|---|---|
| | Exp . | ANSYS | Diff% | Exp. | ANSYS | Diff. % |
| Beam 1 | 102.6 | 109.2 | 6.43% | 12 | 10.518 | 12.35% |
| Beam 2 | 133 | 126 | 5.26% | 8.53 | 9.699 | 13.7% |
| Beam 3 | 136.8 | 132 | 3.5% | 8.9 | 8.929 | 0.32% |
| Beam 4 | 146.3 | 134.16 | 8.3% | 9.67 | 9.126 | 5.62% |
| Beam 5 | 125.4 | 124.8 | 0.48% | 9.2 | 8.657 | 5.9% |
| Beam 6 | 98.8 | 103.2 | 4.45% | 6 | 7.489 | 24.81% |
| Beam 7 | 83.6 | 88.8 | 6.22% | 7.2 | 7.359 | 2.21% |
| Beam 8 | 57 | 64.8 | 13.68% | 5.7 | 6.033 | 5.84% |
| | Mean of Diff% | | 6.04% | Mean of Diff% | | 8.84% |

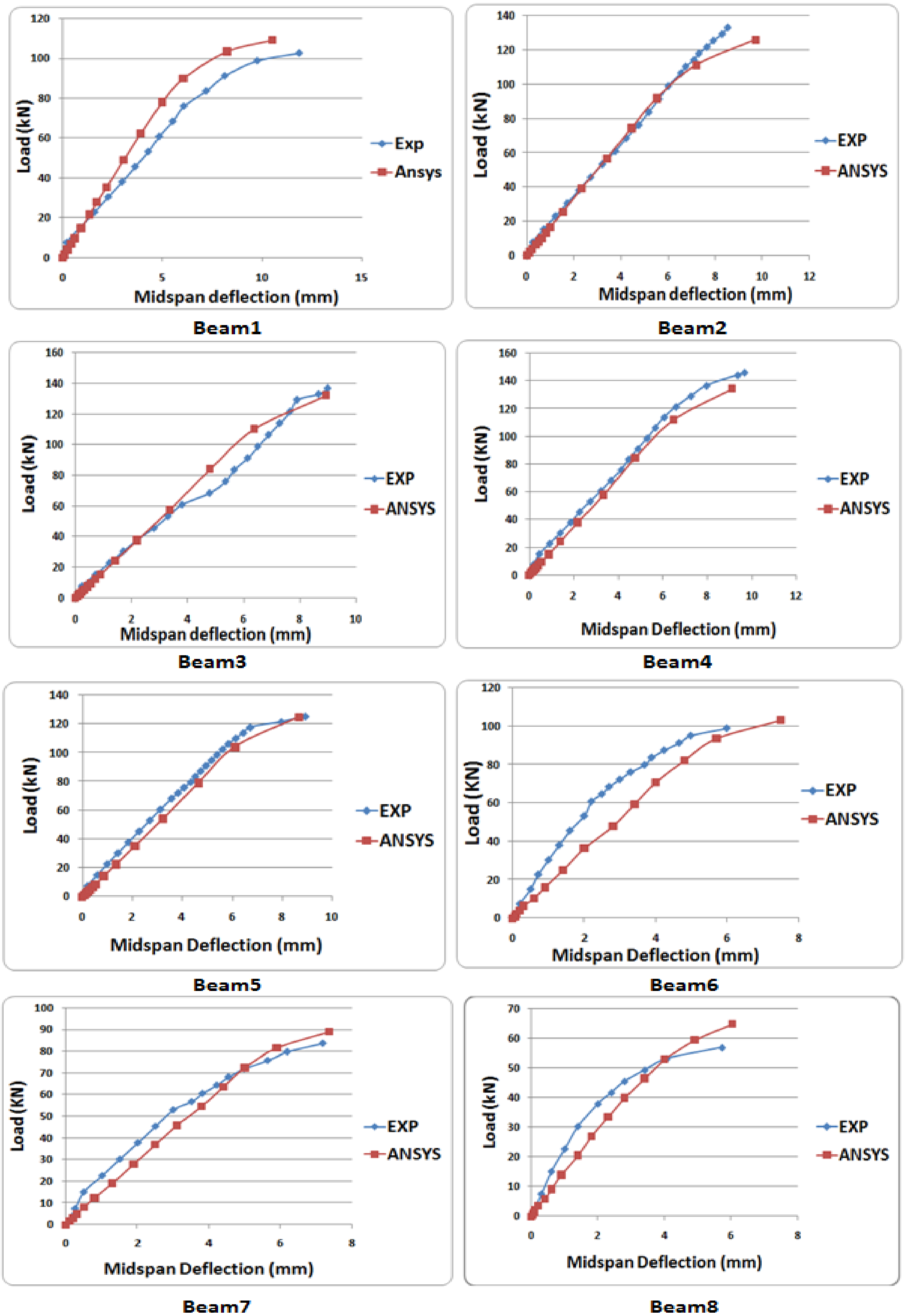


Fig. 12: Finite-element and experimental load~deflection curves for eight tested beams

# CONCLUSION

Based on the experimental and theoretical results , the following conclusions can be drawn:

**a)** Production of SCC mix that satisfies the three fundamental properties (c.g. flowability, passing ability through congested reinforcement , and high segregation resistance ) with moderate cement content and medium compressive strength suitable for most structures becomes possible**.**

**b)** Fructification of the fresh properties of the SCC in improving the performance of the hardened concrete as it furnishes a homogeneous medium free of lumping and segregation, thus raising the degree of integrity with the embedded shear connectors.

**c)** With appropriate shear connection, the steel plate and concrete can work together very well and be treated as fully shear connection.

**d)** Possibility of Using the **"** Strength Method **"** of the ACI-code to accurately analyze structural systems of SCC to obtain the failure load.

**e)** The present finite-element modeling by ANSYS program has sufficient accuracy and high level of reliability to be used for structural analysis purposes especially in the ultimate stage to determine the associated loads and deflection.

**f)** The results show that there is a substantial improvement in the flexural resistance, increasing the flexural stiffness and decreasing the ductility ratio due to thickening steel plate, On contrary, increasing the spacing between shear connectors to 50% had slight effect on the flexural resistance, but subsequent increase of their spacing to 100% had seriously lowered that resistance, The spacing between shear connectors has a primary effect on the average flexural stiffness and ductility ratio. In regard to the steel plate length, , its shortening has reduced the flexural resistance significantly, decreased the average flexural stiffness and has increased the ductility ratio.

# REFERENCE


1) EFNARC, "Specification and Guidelines for Self-Compacting Concrete" May 2005, 31 pp.

2) Roberts, T.M. and Haji-Kazemi, H., "Strengthening of Under-Reinforced Concrete Beams With Mechanically Attached Steel Plates", International Journal of Cement Composites and Lightweight Concrete, Vol.11, No.1, February 1989, pp. 21-27.

3) Abtan, Y.,"Behavior and Ultimate Strength of Reinforced Concrete Beam Strengthened by External Steel Plate", M.Sc. Thesis, Department of Civil Engineering, Al-Mustansiriya University, Baghdad 1997, 98 pp.

4) Al-Saraj, W. K. A., “Composite Behavior of Reinforced Concrete Beams with External Steel Plates”, M.Sc. Thesis, Al-Mustansiriyah University, 2000, 128 pp.

5) Jianguo Nie and Jie Zhao, " Flexural Behavior of Steel Plate-Concrete Composite Beams" Key Engineering Materials Vols. 400-402, 2009, pp. 37-42.

6) Okamura, H., and Ozawa, K., "Mix-Design for Self-Compacting Concrete", Library of JSCE, No.25, June 1995, pp.107-120.

7) المواصفة القياسية العراقية رقم (5) لسنة 1984، "الاسمنت البورتلاندي"، الجهاز المركزي للتقيس والسيطرة النوعية.

8) المواصفة القياسية العراقية رقم (45) لسنة 1984، "ركام المصادر الطبيعية المستعملة في الخرسانة والبناء"، الجهاز المركزي للتقيس والسيطرة النوعية.

9) MBT Degussa Construction Chemicals, "Glenium 51", 06/97 MBT-ME Revised 06/2002, www.mbt-middle-east.com

10) ASTM Designation C39-86, "Compressive Strength of Cylindrical Concrete Specimens",1989 Annual Book of ASTM Standards,American Society for Testing and Materials, Section 4, V.04.02, pp. 20-24.

11) ASTM C293-86, "Standard Test Method for Flexural Strength of Concrete Using Simple Beam with Two Points Loading", Annual Book of ASTM Standard, Vol. 04.02, 1989, pp. 194-196.

12) British Standards Institution, "BS5400: Part 5: Code of practice for design of composite bridges",British Standards Institution, London, 1979, 34 pp.

13) Nilson, A. H., Darwin, D., Dolan, C. W., “Design of Concrete Structures”, 14thEdition, McGraw-Hill, Inc. 2010.

14) "ANSYS Manual", V. 12.1, 2009.

# NOTATION AND ABBREVIATION

**EFNARC:** European Federation of National Trade Associations Representing Concrete.
**ACI** = American Concrete Institute
**SCC** = Self Compacting Concrete
**SPCC** = Steel-Plate Concrete Composite
**Fig**. = Figure
**ANSYS** = Analysis System

**Pcr**: Cracking load
Δ**cr:** Mid span deflection at first crack
**Pu:** Ultimate load
Δ**u:** Mid span deflection at ultimate load
**AFS:** Average flexural stiffness = Pu/Δu
**BJ:** J-ring value